Pinning Modes and Interlayer Correlation in High-Magnetic-Field Bilayer Wigner Solids

Zhihai Wang,[1,2] Yong P. Chen,[1,3,*] L. W. Engel,[1] D. C. Tsui,[3] E. Tutuc,[2,†] and M. Shayegan[3]

[1]*National High Magnetic Field Laboratory, 1800 East Paul Dirac Drive, Tallahassee, Florida 32310, USA*

[2]*Department of Physics, Princeton University, Princeton, New Jersey 08544, USA*

[3]*Department of Electrical Engineering, Princeton University, Princeton, New Jersey 08544, USA*

(Received 30 November 2006; published 26 September 2007)

We report studies of pinning mode resonances in the low total Landau filling (ν) Wigner solid of a series of bilayer hole samples with negligible interlayer tunneling and with varying interlayer separation d. Comparison of states with equal layer densities (p, p) to single layer states $(p, 0)$ produced *in situ* by biasing, indicates that there is interlayer quantum correlation in the solid at small d. Also, the resonance frequency at small d is decreased just near $\nu = 1/2$ and $2/3$, indicating the importance in the solid of correlations related to those in the fractional quantum Hall effects.

DOI: 10.1103/PhysRevLett.99.136804 PACS numbers: 73.43.Jn, 71.70.Di, 73.43.Lp

Bilayers, pairs of closely spaced sheets of carriers, owing to the additional layer degree of freedom, exhibit a variety of states not present in single layer two-dimensional carrier systems. For example, at total filling factors ν of 1 [1–3] and $1/2$ [4–6], bilayers with negligible interlayer tunneling exhibit the celebrated quantum Hall liquid states, whose existence depends on interlayer quantum correlation, in the sense of wave functions spreading coherently between layers even when interlayer tunneling is essentially negligible. At smaller ν, these same bilayers (at least when disorder is small enough) also form bilayer Wigner crystal (BWC) states [7–9], which are of fundamental interest as prototypical correlated solids. Here we present experimental evidence that some aspects of the interlayer quantum correlations found in the liquid states carry over into the solid BWC states.

Theories [10–12] of idealized disorder-free systems have predicted a number of distinct BWC phases. The relative importance of interlayer and intralayer interaction is crucial in these theories and is measured by the ratio d/a, where d is the center-to-center layer separation, $a = (2\pi p)^{-1/2}$ is the mean in-plane carrier spacing, and p is the carrier density per layer. A one-component triangular lattice is expected at small enough d/a, with one carrier, evenly and coherently spread between the two layers, at each lattice site and is an easy plane pseudospin ferromagnetic BWC (FMBWC), where, as usual in descriptions of bilayer states, the pseudospin specifies the layer. Interlayer-staggered two-component lattices occur at larger d/a and, without interlayer tunneling, are pseudospin antiferromagnetic BWCs (AFMBWCs), with carriers essentially completely in one layer alternating with those completely in the other. Multiple staggered two-component phases are predicted, including square and rectangular lattices. For $d \gg a$, the intralayer interaction dominates, so the layers are simply triangular lattices like single layer Wigner crystals but interlayer-staggered.

Wigner crystals in real samples, bilayer or single layer, are pinned by disorder, and so are insulators. Pinning also produces a striking microwave or rf conductivity resonance, or "pinning mode," which is a collective oscillation of the carriers about their pinned positions. Pinning mode resonances of single layers have been studied experimentally [13–17] and theoretically [18–20] and have proven to be valuable for obtaining information about single layer, pinned Wigner solids. The resonance frequency always increases as the disorder strength increases and is also sensitive [18–20] to the correlation length of the effective disorder, which takes into account the spread of the carrier wave functions. Pinning modes of bilayers [21] have also been observed.

We present a systematic study of the pinning mode in a series of bilayer samples, which have negligible interlayer tunneling and widely varying layer separations. For comparison with work on the $\nu = 1$ excitonic condensate [1–3], we present the effective layer separation as $\tilde{d} = d/l_B = 2^{1/2}d/a$, where l_B is the magnetic length at $\nu = 1$ in the balanced state. To isolate effects of interlayer interaction or quantum correlation, we compare spectra of balanced states [layer carrier densities (p, p)] to those of single layers [layer densities $(p, 0)$] created *in situ* by depleting one of the layers. Denoting the resonance frequencies in these states by f_{pp} and f_{p0}, respectively, we examine the ratio $\eta = f_{pp}/f_{p0}$ for the samples. We emphasize that this ratio is taken to remove the effects of sample-to-sample disorder variation. $\eta = f_{pp}/f_{p0}$ vs $\tilde{d}$ has a distinct minimum at $\tilde{d} \approx 1.8$ whose interpretation is in terms of two competing effects, which, respectively, tend to lower and raise η as $\tilde{d}$ decreases: (1) turn-on of the interlayer interaction on going from the $(p, 0)$ single layer to the (p, p) BWC and (2) enhancement [22] of the effective pinning disorder in the (p, p) state relative to that in the $(p, 0)$ state *only when the* (p, p) *state is an interlayer quantum correlated FMBWC*. Of importance as well, and present only for small $\tilde{d}$, are distinct dips in f_{pp} vs B, around $\nu = 1/2$ or $2/3$, demonstrating the effect, within the low ν BWC insulator, of correlations present in the fractional quantum Hall effect (FQHE) states.

The samples, described in Table I, are GaAs double quantum well hole systems grown on (311)A substrates. Each wafer has a pair of 150 Å GaAs wells, which are separated by AlAs barriers for $d \leq 300$ Å, and a combination of AlAs and AlGaAs for $d > 300$ Å. All of the wafers are designed to have negligible interlayer tunneling. $\mathrm{Re}(\sigma_{xx})$ vs B traces, such as those in Fig. 1(b), show a dip around $\nu = 1$ for the lower $\tilde{d}$ samples. The absence of this dip for $\tilde{d} \geq 1.69$ nearly agrees with earlier results [1,3], in which the $\nu = 1$ state is present for $\tilde{d} \leq 1.8$.

We performed microwave measurements using a method that has been described earlier [15–17]. A coplanar waveguide (CPW) transmission line, on top of the sample, couples capacitively to the bilayer, as shown schematically in Fig. 1(a). The CPW has a narrow, driven center conductor separated from grounded side planes by slots of width W. The measurements proceed in a high frequency, low loss limit of the CPW, in which the microwave field is only slightly perturbed by the conductivity of the bilayer. In this case, the in-plane microwave electric field (1) is mainly confined to the region immediately under the slots and (2) is essentially the same in both layers. We calculated the real part of diagonal conductivity from the transmitted power P using a formula valid in this limit, when reflections are minimal: $\mathrm{Re}(\sigma_{xx}) = -W|\ln(P/P_0)|/2Z_0L$, where P_0 is the transmitted power with all carriers depleted from the bilayer, $Z_0 = 50\ \Omega$ is the characteristic impedance calculated for the CPW geometry with $\sigma_{xx} = 0$, and L is the length of the CPW. The data, all taken around 60 mK, were obtained in the low power limit, in which further power reduction did not affect the measured $\mathrm{Re}(\sigma_{xx})$. A voltage applied between a back gate and contacts to both layers was used to control the layer densities.

The microwave measuring method precludes the use of front (top) gates to allow independent tuning of the top and bottom layer densities. A metal film too close to the slots would effectively shield the bilayer from the required in-plane microwave field. Hence, a balanced state is produced only by tuning the back gate voltage and can for each cooldown be produced at only one density. For comparison with balanced bilayer states with layer densities (p, p), we realize a single layer state $(p, 0)$ *in situ*, by reducing the total density, as evaluated from quantum Hall features, by 50% from that in the balanced state.

Figure 1(b) shows $\mathrm{Re}(\sigma_{xx})$ vs B for M465 and M433, in their balanced states, measured at $f = 200$ MHz. It shows that the main features observed [2,8,23] in dc transport are still readily observable with the transmission line. M465, with $\tilde{d} \approx 1.56$, exhibits the $\nu = 1$ IQHE, while M433, with $\tilde{d} \approx 1.8$, does not. We used rf traces such as these to assess the total density and also to find the balanced states, by adjusting the back gate voltage, to minimize the strength of the $\nu = 1$ feature (for M440, M465, and M417) [8] or to minimize the hysteresis in B of quantum Hall states (for M433, M436, M443, and M453) [23].

Figure 1(c) illustrates the evolution with B (and ν) of the spectra of M465 in its balanced state. Parameters from the spectra, f_{pp} and Q (f_{pp} divided by full width at half maximum linewidth), are plotted vs ν in Fig. 1(d). In M465, and the other two samples (M417 and M440) with the smallest $\tilde{d}$, the resonance is present for ν just below the $\nu = 1$ quantum Hall minimum and sharpens dramatically

TABLE I. Sample parameters in balanced states: center-to-center well separation (d), density per layer (p), and effective separation $\tilde{d} = d/l_B$, where $l_B = (4\pi p)^{-1/2}$ is the magnetic length at total filling factor $\nu = 1$. The two p, $\tilde{d}$ for M417 and M433 are from different cooldowns. The last column states whether a minimum in $\mathrm{Re}(\sigma_{xx})$ vs magnetic field at $\nu = 1$ is present.

Wafer	d (Å)	p (10^{10} cm^{-2})	$\tilde{d}$	$\nu = 1$ QHE
M440	225	3.00	1.38	Yes
M465	230	3.65	1.56	Yes
M417	260	2.70	1.51	Yes
		3.05	1.61	Yes
M433	300	2.52	1.69	No
		2.85	1.80	No
M436	450	2.40	2.47	No
M443	650	2.85	3.89	No
M453	2170	5.3	18	No

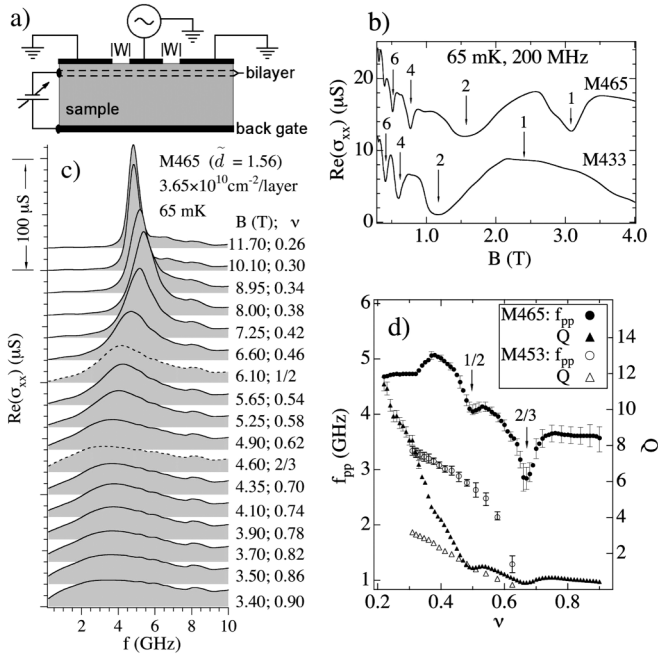

FIG. 1. (a) Magnified cross section, not to scale, through the transmission line and sample. (b) Real part of diagonal conductivity $\mathrm{Re}(\sigma_{xx})$ vs magnetic field B for M465, and M433, in their balanced states. Total Landau filling factors ν are marked. (c) $\mathrm{Re}(\sigma_{xx})$ vs frequency f for M465 in its balanced state, for many B (or ν). Spectra are vertically displaced proportional to ν and shaded downward to their zeros. (d) Peak frequency f_{pp} and Q vs ν (Q is f_{pp} divided by full width at half maximum).

as ν decreases below about 0.5, so that the Q vs ν curve in Fig. 1(d) shows a change of slope at that filling.

In the samples with $\tilde{d} \geq 1.69$, the resonance appears as ν decreases below about 0.6, with gradually increasing f_{pp} and Q. This resonance development is typical of that seen at the same per-layer filling, previously [16] in low density p-type single layers, and in the present samples in their single layer $(p, 0)$ states. f_{pp} and Q for M453, which has the largest $\tilde{d}$ and therefore essentially independent layers, are plotted vs ν in Fig. 1(d) as well.

M465 shows clear dips in f_{pp} vs ν around $\nu = 1/2$ and $2/3$ in the plot in Fig. 1(c). (M417 and M440 have weak dips in f_{pp} at $2/3$ or $1/2$, but the dips in those samples are not nearly as clear as in M465, possibly due to the higher p of M465.) The resonance is well-developed at these fillings, which are well within the insulating phase of this sample, so we do not interpret the dips as FQHE liquid ground states [4–6,24] but rather as evidence that some of the correlations related to the FQHE are present in the pinned BWC. In general, as Wigner solid moduli increase, the resonance frequency decreases [17–20]; hence, the dips in f_{pp} correspond either to *increases* in BWC stiffness or to decreases in the effective carrier-disorder interaction. The $1/2$ FQHE has no analog in the single layer case and is interlayer-correlated, though the $2/3$ feature can be explained with intralayer correlation. Composite fermion theories [25,26] have predicted that correlations related to the FQHE are important in single layer, low ν Wigner solids.

The main results of this Letter follow from direct comparison, for each sample, of the balanced (p, p) and single layer $(p, 0)$ states. Spectra from these pairs of states are shown for four samples, at $B = 10$ T in Figs. 2(a)–2(d). The bilayer spectra are shown as solid lines, and the single layer spectra are dashed lines. Re(σ_{xx}) from the single layer states is doubled to facilitate comparison. The M453 spectra in Fig. 2(d) are nearly identical, as expected for independent layers, and not surprising considering the large $\tilde{d} \approx 18$ for that sample. Important for the interpretation below, the nearly identical spectra also indicate that the disorder statistics relevant to the pinning mode are essentially the same in the top and bottom wells. The disorders of the two layers should likewise be similar for all of the samples, since they all had similar growth characteristics, such as asymmetrical doping and interfacial compositions.

Hence, we interpret the differences between the (p, p) and $(p, 0)$ spectra in Figs. 2(a)–2(d) as due to changes in interlayer interaction and correlation. Relative to the $(p, 0)$ spectra, the (p, p) spectra shift slightly to lower frequency as $\tilde{d}$ decreases down to 2.47, as shown in Fig. 2(c). At $\tilde{d} \approx 1.8$, though, for M433 as shown in Fig. 2(b), the (p, p) spectrum is markedly shifted downward in frequency and is stronger and sharper. But decreasing $\tilde{d}$ further (even through a different cooldown of the same M433 sample) reduces the downward shift of f_{pp} relative to f_{p0}, though

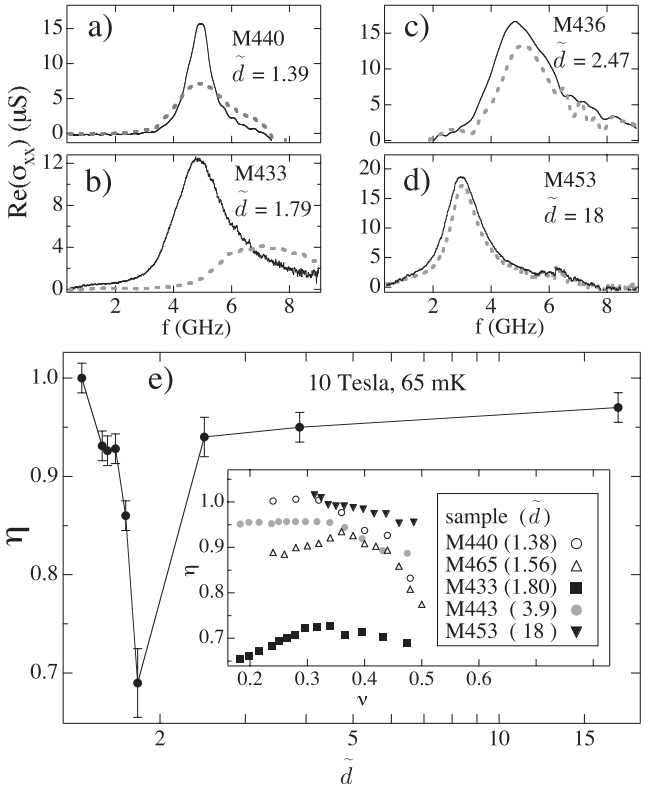

FIG. 2. (a)–(d) For four samples, the spectrum in the balanced state with layer densities (p, p) (solid line) is plotted along with the spectrum [with the measured Re(σ_{xx}) multiplied by two] of the single layer state $(p, 0)$ (dotted line), all at magnetic field $B = 10$ T. (e) $\eta = f_{pp}/f_{p0}$ at 10 T vs $\tilde{d} = d(4\pi p)^{1/2}$, where f_{pp}, f_{p0} are the peak frequencies for the (p, p) and $(p, 0)$ states, respectively, and d is layer separation. Inset: η vs ν, the total filling in the bilayer (p, p) state, for five samples.

the (p, p) spectra remain much sharper than the $(p, 0)$ spectra, as seen in Fig. 2(a). To summarize for all of the samples, Fig. 2(e) shows the ratio $\eta = f_{pp}/f_{p0}$ vs $\tilde{d}$; this curve has a striking minimum at $\tilde{d} \approx 1.8$. The inset in Fig. 2(e) is a graph of η vs ν, the total filling of the (p, p) states, for several samples. This graph shows that the minimum in η vs $\tilde{d}$ remains, whether B or ν is fixed, as long as $\nu \lesssim 0.5$.

We will need to interpret the η vs $\tilde{d}$ curve as a result of two competing effects. The first effect is driven by carrier-carrier interaction and must be present in any weakly pinned Wigner crystal, bilayer or single layer. In this effect, when carrier-carrier interaction energy density is increased, by decreasing carrier spacing (or increasing their overall density), the resonance frequency decreases. In single layers at fixed B, at which the resonance is well-developed, as carrier density n_s is decreased, the peak frequency $f_{\rm pk}$ always increases and the resonance broadens. Typically [15,17], $f_{\rm pk} \propto n_s^{-\gamma}$, with $\gamma \approx 3/2$ for higher n_s giving way to $\gamma \approx 1/2$ at lower n_s; the present samples in single layer states all have $\gamma \approx 1/2 \pm 10\%$. The interpretation in weak pinning [17–20] of the increase of $f_{\rm pk}$

with decreasing n_s is that reduction of carrier-carrier interaction (i.e., the crystal stiffness) causes the carriers essentially to fall more deeply into the impurity potential. This increases the pinning energy per carrier, the restoring force on the carriers, and hence f_{pk}.

In bilayers, the carrier-carrier interaction effect produces $\eta = 1$ in the large $\tilde{d}$ limit, with η monotonically decreasing with decreasing $\tilde{d}$ to $\eta = 2^{-\gamma}$, analogous to doubling the density of a single layer. For $\gamma = 1/2$, $\eta = 2^{-\gamma} \approx 0.71$, in agreement with the minimum η, for $\tilde{d} = 1.8$ in Fig. 2(e). Since each η is a ratio from a single cooldown of a single sample, the carrier-carrier interaction effect would have to produce a monotonic decrease in η with decreasing $\tilde{d}$ *regardless of the expected variation of overall disorder from sample to sample.* Hence, a second, competing effect is required to interpret the data.

We interpret the decrease of η with decreasing $\tilde{d}$, for $\tilde{d} \geq 1.8$, as due to the carrier-carrier interaction effect, within an AFMBWC. The sharp increase in η as $\tilde{d}$ goes below 1.8 and hence requires an explanation other than the carrier-carrier interaction effect. Transitions between different types of AFMBWC are predicted by the theories [10–12], and, if $\tilde{d}$ is near a transition, the BWC can conceivably soften (multiple low energy arrangements become possible), producing some increase of η around particular $\tilde{d}$. It is not likely, though, that, even around a transition between AFMBWC phases, η would be as close to unity as it is in Fig. 2(e) at the smallest $\tilde{d}$ values.

To go beyond the carrier-carrier interaction effect, the carrier wave functions must significantly differ in the (p, p) and $(p, 0)$ states, to enhance the pinning in (p, p). The second competing effect that we use to explain η vs $\tilde{d}$ is driven by interlayer correlation, is present only for an FMBWC (p, p) state, and was considered theoretically by Chen [22]. Chen found that in an FMBWC pinning is enhanced when there is disorder that is spatially correlated in the planes of the top and bottom layers. At sites where impurities or interfacial features induce local interlayer tunneling [2], such spatial correlation would naturally result. When this bilayer-state disorder enhancement is considered [22] along with the competing carrier-carrier interaction effect, η as large as $2^{1-\gamma}$ is possible, so the transition to an FMBWC is sufficient to explain the increase of η with decreasing $\tilde{d}$ seen in Fig. 2(e) for $\tilde{d} \lesssim 1.8$. Even within the FMBWC, an increase of η as $\tilde{d}$ decreases is expected, since the smaller $\tilde{d}$ would increase the interlayer spatially correlated component of effective disorder.

The data then indicate that $\tilde{d}^*$, the critical $\tilde{d}$ below which the FMBWC is present, is around 1.8. Theories with small but finite tunneling predict smaller $\tilde{d}^*$, around 0.4 [10,11]. A possible explanation of the discrepancy lies in the increased pinning experienced by the FMBWC, since the pinning energy can stabilize the FMBWC against the more weakly pinned AFMBWC phases that succeed it at larger $\tilde{d}$. It is likely that pinning energy plays a role in stabilizing single layer Wigner crystals against the FQHE liquid at high fillings [27] and against melting at elevated temperatures [14]. A possible clue to the presently estimated $\tilde{d}^* \approx 1.8$ is that it is close to the maximal $\tilde{d}$ values below which the interlayer correlated quantum Hall states at $\nu = 1$ and $1/2$ exist, respectively: $\tilde{d} \approx 1.8$ [1,3] and 2 [4].

In summary, our systematic studies of pinning modes of BWC have found effects of interlayer interaction and give evidence for BWC interlayer correlations in which the wave function of a carrier spreads evenly between the two layers. Correlations related as precursors to the bilayer $1/2$ and $2/3$ FQHEs are also present in the BWC.

We thank N. Bonesteel, H. A. Fertig, and Kun Yang for discussions and acknowledge the support of AFOSR. Z. W. was supported by DOE Grant No. DE-FG02-05ER46212. NHMFL is supported by NSF Grant No. DMR-0084173, the State of Florida, and DOE.

*Present address: Purdue University, West Lafayette, IN, USA.

†Present address: University of Texas, Austin, TX, USA.

[1] M. Kellogg *et al.*, Phys. Rev. Lett. **93**, 036801 (2004).
[2] E. Tutuc, M. Shayegan, and D. A. Huse, Phys. Rev. Lett. **93**, 036802 (2004).
[3] I. B. Spielman *et al.*, Phys. Rev. Lett. **84**, 5808 (2000); **87**, 036803 (2001).
[4] J. P. Eisenstein *et al.*, Phys. Rev. Lett. **68**, 1383 (1992).
[5] Y. W. Suen *et al.*, Phys. Rev. Lett. **68**, 1379 (1992).
[6] Y. W. Suen *et al.*, Phys. Rev. Lett. **72**, 3405 (1994).
[7] H. C. Manoharan *et al.*, Phys. Rev. Lett. **77**, 1813 (1996).
[8] E. Tutuc *et al.*, Phys. Rev. Lett. **91**, 076802 (2003).
[9] S. Faniel *et al.*, Phys. Rev. Lett. **94**, 046802 (2005).
[10] S. Narasimhan and T. L. Ho, Phys. Rev. B **52**, 12 291 (1995).
[11] L. Zheng and H. A. Fertig, Phys. Rev. B **52**, 12 282 (1995).
[12] G. Goldoni and F. M. Peeters, Phys. Rev. B **53**, 4591 (1996).
[13] See G. Sambandamurthy *et al.*, Solid State Commun. **140**, 100 (2006) for a brief review.
[14] Yong P. Chen *et al.*, Nature Phys. **2**, 452 (2006).
[15] P. D. Ye *et al.*, Phys. Rev. Lett. **89**, 176802 (2002).
[16] C.-C. Li *et al.*, Phys. Rev. Lett. **79**, 1353 (1997).
[17] C.-C. Li *et al.*, Phys. Rev. B **61**, 10 905 (2000).
[18] R. Chitra, T. Giamarchi, and P. Le Doussal, Phys. Rev. Lett. **80**, 3827 (1998); Phys. Rev. B **65**, 035312 (2001).
[19] H. A. Fertig, Phys. Rev. B **59**, 2120 (1999).
[20] M. M. Fogler and D. A. Huse, Phys. Rev. B **62**, 7553 (2000).
[21] J. B. Doveston *et al.*, Physica (Amsterdam) **12E**, 296 (2002).
[22] Yong P. Chen, Phys. Rev. B **73**, 115314 (2006).
[23] E. Tutuc *et al.*, Phys. Rev. B **68**, 201308(R) (2003).
[24] A. R. Hamilton *et al.*, Phys. Rev. B **54**, R5259 (1996).
[25] R. Narevich, G. Murthy, and H. A. Fertig, Phys. Rev. B **64**, 245326 (2001).
[26] C.-C. Chang, G. S. Jeon, and J. K. Jain, Phys. Rev. Lett. **94**, 016809 (2005).
[27] R. Price *et al.*, Phys. Rev. B **48**, 11 473 (1993).